Eur. Phys. J. D **13**, 245–253 (2001)

THE EUROPEAN PHYSICAL JOURNAL D

EDP Sciences

Importance of lattice contraction in surface plasmon resonance shift for free and embedded silver particles

W. Cai[1,a], H. Hofmeister[1,b], and M. Dubiel[2]

[1] Max Planck Institute of Microstructure Physics, Weinberg 2, 06120 Halle, Germany
[2] Martin Luther University of Halle-Wittenberg, Department of Physics, Friedemann-Bach-Platz 6, 06108 Halle, Germany

Received 26 July 2000 and Received in final form 14 September 2000

Abstract. The size evolution of the surface plasmon resonance was investigated for free and embedded silver particles between about 2 to 10 nm in size. The crystal lattice of such particles as analyzed by high resolution electron microscopy show linear contraction with reciprocal particle size. Based on this, a model was presented by combining the lattice contraction of particles and the free path effect of electrons to predict the size evolution of the resonance. The results reveal a contribution of the lattice contraction to the resonance shift according to a roughly linear relation that changes slightly with particle radius (> 1.0 nm) and surrounding media. This surface plasmon resonance shift proceeds linearly with reciprocal size for Ag particles in vacuum and argon, but for Ag particles embedded in glass it appears to be independent of the radius down to nearly 1 nm. All predictions are quantitatively compared to previously reported experimental data and a good agreement is obtained. An unusual red-shift observed for Ag particles in glass may be attributed to a thermal expansion mismatch induced lattice dilatation.

PACS. 61.46.+w Clusters, nanoparticles, and nanocrystalline materials – 78.40.-q Absorption and reflection spectra: visible and ultraviolet – 78.66.-w Optical properties of specific thin films, surfaces, and low-dimensional structures

1 Introduction

The optical absorption of small particles has been investigated for a long time. The well-known surface plasmon resonance for noble metal particles has also been extensively investigated theoretically and experimentally [1–3]. The spectral position $\hbar\omega_0$ of the absorption peak for a metallic sphere was calculated by Mie at the beginning of 20th century [4] and is given by

$$\varepsilon(\omega_0) = -2\varepsilon_{\mathrm{m}} \tag{1}$$

where $\varepsilon(\omega)$ is the frequency-dependent dielectric function (real part) of the metal, ω the frequency of incident light, ω_0 the Mie resonance frequency and ε_{m} the dielectric constant of the surrounding medium for the metal particle. This relationship is valid if the particle size is small enough for the quasistatic approximation to be applied. However, the situation is not so clear for even smaller particles (radii smaller than 5 nm). Numerous experiments performed on silver (Ag) particles have pointed out the sensitivity of the size evolution of the Mie frequency on the surrounding matrix and the size range studied [5,6]. Some of them yielded a shift of the resonance peak towards lower energy (red shift) for radii smaller than 4 nm, with respect to the frequency ω_0 given by equation (1) [7–10]. Other experiments showed a blue shift ranging from the order of the experimental dispersion [11] up to 0.2 eV for radii below 4 nm [12,13]. Several theoretical explanations have been proposed to interpret this contradictory behavior.

Roughly, the size evolution of the Mie frequency is the net result of the competition between two opposite trends. The red shift is induced by the so-called spillout effect of free electrons [14] and the blue shift results from the increasing importance of the skin region of ineffective screening as the particle radius decreases, which was phenomenologically described by a two-region (skin and core regions of a particle) dielectric model, assuming that the continuous polarizable medium mimics the screening by the core electrons [15–18]. In addition, Genzel, Martin and Kreibig [11] obtained the dielectric function by considering the quantum degeneracy. Cocchini, Bassani and Bourg [19] introduced a soluble tight-binding model. Wen Chu Huang and Juh Tzeng Lue [20] presented the quantum sphere model. Lerme *et al.* applied time-dependent-local density approximation within the context of jellium sphere calculations involving concentric, spherically symmetric dielectric media [21,22]. Alternatively, electron stimulated excitation of plasmon resonances have been extensively studied by electron energy loss spectroscopy [23–28]. Generally, the quantized energy levels for metallic nanoparticles of a few nm diameter will form a discrete electronic structure, but previous experiments have

[a] *Permanent address*: Institute of Solid State Physics, Academia Sinica, Hefei 230031, People's Republic of China.
[b] e-mail: `hof@mpi-halle.mpg.de`

shown that normal metal properties are still present for noble metals such as Ag [29] or Au [30] down to particle sizes of about 2 nm. According to Smithard [8], the free path effect of electrons should even hold for particle sizes of about 1 nm. However, the origins of the Mie resonance shift are still controversial and not clarified completely.

In fact, a shift of the resonance position with particle size variation may result from several different effects, such as changes of optical interband transitions, changes of electronic band structure, changes of the effective mass of the conduction electrons and changes of lattice constants etc., as listed in reference [31]. It is evident that the relative importance of these effects for the change of the Mie resonance is different, depending on the experimental conditions and materials. In previous extensive works, ones mainly emphasized the core electron contribution and not the effect induced by the possible change of the free electron plasma frequency ω_{P}, which is usually taken as a constant, independent of the particle size. Actually, in some cases, when the metal particles are small enough, the change of ω_{P} due to the particle size variation plays an important part in shift of the Mie resonance as it will be treated in the following sections. It is well-known that the lattice constant of small particles is different from the bulk, owing to the existence of surface or interface stress. Obviously, the variation of lattice constants will result in a change of the electron density in the particles, and hence the change of ω_{P} and shift of the Mie resonance. However, an investigation of the effect of lattice contraction, due to reduction of particle size, on the Mie resonance has not been reported so far, to our knowledge. Although mentioned in the literature [29,31,32], only thermal contraction was considered in calculations [29].

In this paper, combining the experimental results of lattice constant variation with particle size, based on the classical theory including the free path effect of electrons, which is the strongest of all known particle-size effects for realistic metals [31,32], we investigate the importance of lattice contraction for the shift of the resonance position of free, nearly spherical silver particles and those embedded in argon and glass (weakly interacting with metals) in the range of 2 to 10 nm diameter. It is shown that the lattice contraction induced by surface stress plays an important part in the shift of the surface plasmon resonance. The results clearly show that the observed size trends for the free and embedded silver particles can be explained by the classical theory in combination with the lattice contraction and free path effect.

2 Theory

2.1 Model

According to the Mie theory, the extinction cross-section σ_{abs} is given by the dipole absorption

$$\sigma_{\mathrm{abs}} = \frac{18\pi\varepsilon_{\mathrm{m}}^{3/2}V_0}{\lambda}\frac{\varepsilon_2(\omega)}{[\varepsilon_1(\omega)+2\varepsilon_{\mathrm{m}}]^2+\varepsilon_2^2(\omega)} \tag{2}$$

in the case of metal particles of radii R much less than wavelength λ, where V_0 is the spherical particle volume and $\varepsilon(\omega)=\varepsilon_1(\omega)+\mathrm{i}\varepsilon_2(\omega)$. The dipole resonance frequency is determined by the condition $\varepsilon_1(\omega)=-2\varepsilon_{\mathrm{m}}$, namely equation (1), provided $\varepsilon_2(\omega)$ is not too large and does not vary much in the vicinity of the resonance, which is reasonable when the particle radius is larger than ~ 1 nm for the silver case. Taking account of the free electron contribution parameterized as a Drude-Sommerfeld formula, the dielectric function $\varepsilon(\omega)$ is given by

$$\varepsilon(\omega) = \varepsilon_{\mathrm{b}}(\omega) + 1 - \frac{\omega_{\mathrm{P}}^2}{\omega^2+\mathrm{i}\omega\tau^{-1}} \tag{3}$$

where $\varepsilon_{\mathrm{b}}(\omega)$ is the core electron dielectric function, and τ the relaxation time. The plasma frequency $\omega_{\mathrm{P}} = \left(ne^2/\varepsilon_0 m_{\mathrm{eff}}\right)^{1/2}$ depends on the electron density n and on the proper electron effective mass m_{eff}. For metals with face-centered cubic structure, it can be rewritten as

$$\omega_{\mathrm{P}} = \left(4e^2/a^3\varepsilon_0 m_{\mathrm{eff}}\right)^{1/2} \tag{4}$$

where a and ε_0 are lattice constant and vacuum dielectric constant, respectively, and e is the electronic charge. So we have the resonance frequency $\omega_{\mathrm{r}}(R)$ according to equation (1)

$$\omega_{\mathrm{r}}^2(R) = \frac{\omega_{\mathrm{P}}^2}{B} - \tau^{-2} \tag{5}$$

where $B = 1 + 2\varepsilon_{\mathrm{m}} + \mathrm{Re}\,\varepsilon_{\mathrm{b}}(\omega)$, Re is the real component. As described in many references [3,21,22], the core electrons have an important influence on the Mie frequency. The great sensitivity of the size evolution to the experimental conditions is found to be closely related to the steep frequency dependence of $\varepsilon_{\mathrm{d}}(\omega)$ near the Mie resonance, expressed in the parameter B. However, in the particle size range considered (about 2 to 10 nm), $\mathrm{Re}\,\varepsilon_{\mathrm{d}}(\omega)$ can be taken being independent of R. The Mie frequency $\omega_{\mathrm{r}}(\infty)$ in the large-size limit is given by

$$\omega_{\mathrm{r}}^2(\infty) = \frac{\omega_{\mathrm{P0}}^2}{B} - \tau_{\mathrm{b}}^{-2} \approx \frac{\omega_{\mathrm{P0}}^2}{B} \tag{6}$$

where ω_{P0} and τ_{b} are the plasma frequency and relaxation time for the bulk, respectively. When the particle size is small enough, however, not only the free path of conduction electrons will be reduced due to the restriction of the particle surface, but also the lattice parameter will be changed owing to the surface stress of free particles or the interface stress of particles embedded in a matrix. This variation of the free path of the electron with the particle radius R is given by [29]

$$\tau^{-1} = \tau_{\mathrm{b}}^{-1} + \frac{AV_{\mathrm{F}}}{R} \tag{7}$$

where V_{F} denotes the Fermi velocity and A includes details of the scattering processes. Direct consequences of the lattice constant variation are the changes of electron density

n, and hence plasmon frequency $\omega_{\rm P}$, as well as Fermi velocity $V_{\rm F}$. Considering the cubic structure and combining equations (4, 5, 7) we have

$$\omega_{\rm r}^2(R) = \frac{\omega_{\rm P0}^2}{B}\frac{a_0^3}{a^3} - \tau_{\rm b}^{-2} - \frac{AV_{\rm F0}}{R}\left(\frac{a_0}{a}\right)\left[2\tau_{\rm b}^{-1} + \frac{AV_{\rm F0}}{R}\left(\frac{a_0}{a}\right)\right] \quad (8)$$

where a is the lattice constant for particles and a_0 and $V_{\rm F0}$ are the corresponding values for the bulk. Obviously, the lattice contraction influences the Mie frequency in two opposite aspects. On the one hand, the contraction increases the volume plasma frequency $\omega_{\rm P}$, which leads to a blue-shift of the Mie frequency; on the other hand, it increases the Fermi velocity and hence intensifies the free path effect, which results in a red-shift. Both are partially counteracting.

Since equation (8) is somewhat cumbersome, we give below only approximate expressions valid in a restricted range of parameters, from which the physical meaning appears more clearly. Taking into account $a_0/a \approx 1 - \Delta a/a_0$ and $(a_0/a)^3 \approx 1 - 3\Delta a/a_0$, together with $\tau_{\rm b}^{-1} \ll \omega_{\rm P0}$, we obtain

$$\omega_{\rm r}^2(R) \approx \omega_{\rm r}^2(\infty)\left[1 - \frac{3\Delta a}{a_0}\right] - \left[\frac{AV_{\rm F0}}{R}\left(1 - \frac{\Delta a}{a_0}\right)\left(2\tau_{\rm b}^{-1} + \frac{AV_{\rm F0}}{R}\left(1 - \frac{\Delta a}{a_0}\right)\right)\right]. \quad (9)$$

Further, on the assumption of a cubic lattice and a spherical shape, the lattice contraction of a particle can be described by using the surface stress f [33], or the interface stress for embedded particles, respectively, as

$$\frac{\Delta a}{a_0} = -\frac{2}{3}\frac{Kf}{R} \quad (10)$$

where K is the compressibility. Therefore we have

$$\omega_{\rm r}^2(R) = \omega_{\rm r}^2(\infty) + \Delta\omega_{\rm rL}^2 - \Delta\omega_{\rm rP}^2 \quad (11)$$

in which

$$\Delta\omega_{\rm rL}^2 = \omega_{\rm r}^2(\infty)\frac{2Kf}{R} \quad (12)$$

i.e. the contribution to the resonance frequency change induced by lattice contraction and

$$\Delta\omega_{\rm rP}^2 = \frac{AV_{\rm F0}}{R}\left(1 + \frac{2}{3}\frac{Kf}{R}\right) \times \left[2\tau_{\rm b}^{-1} + \frac{AV_{\rm F0}}{R}\left(1 + \frac{2}{3}\frac{Kf}{R}\right)\right] \quad (13)$$

namely, the contribution induced by the free path effect. Obviously, the value of parameter A determines the magnitude of the free path effect. It has been extensively investigated [3] and will not be further discussed in this paper. Equation (11) shows that the Mie frequency is only a function of the particle radius. It will be altered by lattice contraction and free path effect which both are associated with the particle radius. If the lattice parameter diminishes with decreasing particle size, which is usually expected, the lattice contraction will lead to a blue-shift of the Mie frequency, in contrast to the free path effect which results in a red-shift when decreasing the particle size. The size evolution of the Mie frequency is thus the net result of the competition between both opposite trends, showing blue shift, red-shift or quasi-size-independent evolution, which depends on the value and sign of the stress f. If its value is small enough or negative (namely lattice dilatation), a red shift of the resonance should be found.

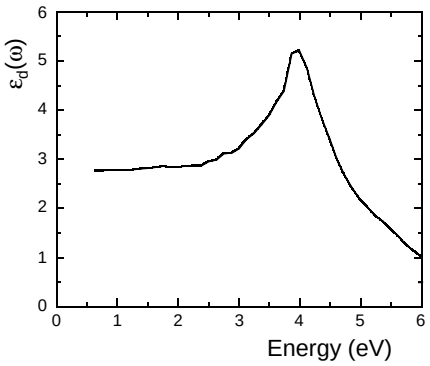

Fig. 1. Spectral dependence of the real part of the core electron dielectric function $\varepsilon_{\rm d}(\omega)$ for silver metal.

2.2 Determination of resonance frequency

It should be pointed out that the parameter B in equations (5, 6, 8) is not really constant. It will vary with the particle size in some implicit form because the Mie frequency $\omega_{\rm r}(R)$ changes with R and the core electron dielectric function $\varepsilon_{\rm d}(\omega)$ is associated with the frequency. Figure 1 shows the spectral dependence of the real component of the complex dielectric function corresponding to the core electrons of silver metal, which was obtained from equation (3) according to the optical constants and related data given by Johnson and Christy [34]. Taking into consideration the errors resulting from the simple parameterization in the third term of equation (3) and the numerical assumptions on $m_{\rm eff}$ and $\tau_{\rm b}$, some authors employed another method to determine the $\varepsilon_{\rm d}(\omega)$ spectra from bulk optical constant data. At first, the imaginary component $\mathrm{Im}\,\varepsilon_{\rm d}$ is obtained by subtracting from the total imaginary component $\mathrm{Im}\,\varepsilon(\omega)$ the free electron contribution parameterized as a Drude-Sommerfeld formula. Then the real component $\mathrm{Re}\,\varepsilon_{\rm d}(\omega)$ is obtained by a Kramers-Kronig analysis [22,35]. However, according to our calculation for silver, both results are in good agreement (see also Fig. 1b in Ref. [36]) in the frequency range studied.

We see that only in the range smaller than 3.0 eV the $\mathrm{Re}\,\varepsilon_{\rm d}$ can approximately be taken as a constant. In the range larger than 3.0 eV, however, $\mathrm{Re}\,\varepsilon_{\rm d}(\omega)$ varies significantly with frequency. Therefore, we should determine the evolution of the Mie frequency with particle size from

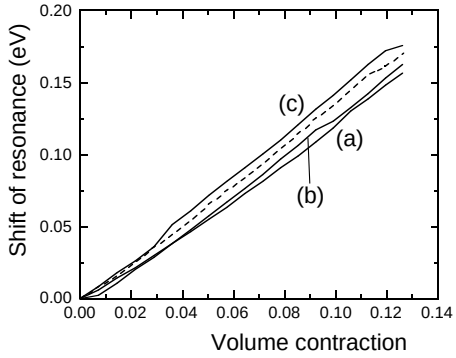

Fig. 2. Contribution of the lattice contraction to the Mie resonance shift for silver particles of $R = 1$ nm in (a) vacuum, (b) argon matrix and (c) glass (solid lines) and for $R = 5$ nm particles in glass (dashed line).

the full expression of equation (8) combined with equation (10). According to the $\varepsilon_{\rm d}(\omega)$ spectrum indicated in Figure 1, for a given R value, we obtain the corresponding Mie frequency $\omega_{\rm r}(R)$ by determining the minimum value of the expression

$$\left|\omega_{\rm r}^2(R) - \omega^2\right|$$

in the whole resonance region, in which $\omega_{\rm r}^2(R)$ is the right side of equation (8).

In addition to the method mentioned above, we can also determine $\omega_{\rm r}(R)$ directly from equation (2) combined with equations (3, 4, 7, 10). Inserting equations (3, 4, 7, 10) into equation (2) yields, according to the optical data presented in reference [34], the Mie resonance absorption spectrum and hence the Mie frequency for a given R value can be obtained.

2.3 Contribution of lattice contraction to the resonance shift

According to the model considerations and determination methods treated above, we calculated the lattice contraction induced peak shift for silver particles of different size and different surrounding medium (weak interaction with metal particles) by using the values $a_0 = 0.40861$ nm, $\tau_{\rm b}^{-1} = 2.70 \times 10^{13}$ s^{-1} [29], $m_{\rm eff} = 0.96 m_0$ [34] (m_0 being the free electron mass), $A = 0.25$ [32], 0.3 [37] and 1.0 [29] as well as $\varepsilon_{\rm m} = 1$, 1.75 [38] and 2.25 for vacuum, argon and glass, respectively. Thus, the values of $\omega_{\rm P0}$ and $V_{\rm F0}$ are obtained to be about 9.1 eV and 1.4×10^{15} nm s^{-1}, respectively. The contribution of lattice contraction to the Mie resonance shift $\Delta\omega_{\rm L}$ is determined from equation (8) [39], by considering the actual lattice parameter a in addition to the free path effect contribution with $a = a_0$. It is found only weakly dependent on the particle size ($R > 1.0$ nm) and the surrounding medium. Figure 2 shows the results for particles of 1 nm radius situated in vacuum, argon and glass, respectively. For comparison, also the contribution of particles of 5 nm radius in glass is included. There exists a roughly linear relation between $\Delta\omega_{\rm L}$ and the volume contraction of silver particles, or

$$\Delta\omega_{\rm L} = C\frac{\Delta V}{V} \tag{14}$$

where $\Delta V/V = (a_0^3 - a^3)/a_0^3$. By linear regression, we obtain $C = 1.44 \pm 0.04$ eV, 1.33 ± 0.03 eV and 1.26 ± 0.02 eV for the surrounding media glass, argon and vacuum, respectively, in the whole particle size range studied with $\Delta V/V < 12\%$.

From equation (8) it seems that high $\varepsilon_{\rm m}$ will result in low $\Delta\omega_{\rm L}$. Actually, however, the opposite is true. As shown in Figure 2, $\Delta\omega_{\rm L}$ is higher in glass than in vacuum and argon for the same amount of volume contraction. As mentioned above, the reason for this difference is the core electron dielectric function $\mathrm{Re}\,\varepsilon_{\rm d}$ being strongly dependent on the frequency ω in the range larger than 3.0 eV. Since the Mie frequency is less than $\omega_{\rm max}$, the maximum frequency of the $\mathrm{Re}\,\varepsilon_{\rm d}$ spectrum, the B value in equation (8) will increase due to the accompanying blue-shift (see Fig. 1) and, in turn, weaken the blue-shift effect. Obviously, the higher the Mie frequency, the weaker the lattice contraction induced blue-shift will be. For a given volume contraction, its contribution to the blue-shift of the Mie resonance is greater in glass than in vacuum and argon because of the lower Mie frequency in glass.

3 Experimental details and results

At this point, in order to confirm the above model, we should know the lattice parameter variation with particle size. The corresponding data have been experimentally determined by high resolution electron microscopy (HREM) for free Ag particles and those embedded in glass. The preparation details were previously described [40].

Here briefly, for free Ag particles, first Ag/silica composite was synthesized from tetraethoxysilane orthosilicate and silver nitrate by sol-gel technique and subsequent drying, calcination in air at 673 K and hydrogen reduction at 623 K. Then the composite was ground and exposed to ultrasonic agitation in propanol to remove the silver particles from the surface of the silica gel. These particles were transferred onto copper microgrids coated with carbon supporting films for electron microscopy analysis. The Ag doped glass was prepared by ion exchange and thermal treatment. The glass is composed of 72% SiO_2, 13.8% Na_2O, 6.5% CaO, 6% MgO (in mol%), and traces of Al_2O_3, K_2O, SO_3 and Fe_2O_3. The silver ions were introduced into the glass matrix by immersing the samples in a mixed $AgNO_3$(2wt%)/$NaNO_3$(98wt%) melt at 673 K for 2 hours or in a $AgNO_3$(5wt%)/$NaNO_3$(95wt%) melt at 673 K for 0.5 hour respectively. Ag particles of different mean sizes precipitated by subsequent annealing at 923 K for 50 hours. The samples were slowly cooled down to room temperature to exclude the generation of additional stress effects. The samples obtained in this way were then cut into pieces, mechanically polished and Ar^+ ion beam etched to obtain thin enough electron-transparent specimens.

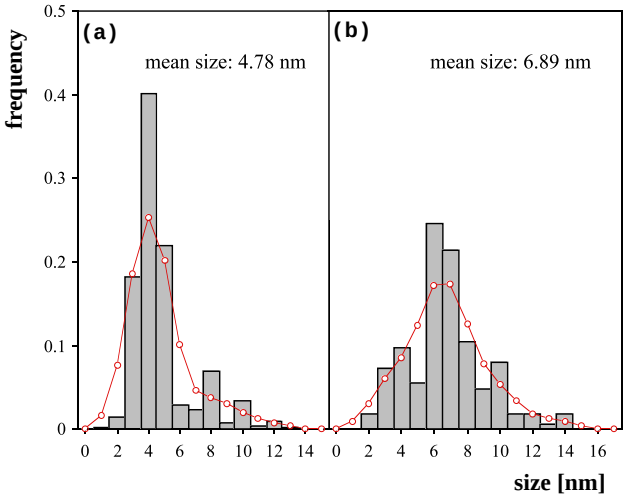

Fig. 3. Size distribution of free silver particles supported on carbon film (a) and silver particles embedded in glass (b).

The structural characterization of the silver particles was performed at room temperature on a JEM 4000EX (operating at 400 kV). Both routes of synthesis mentioned above produced particles of fairly narrow size distribution as shown in Figure 3. It should be noted here, that it is this distribution which allowed to determine the evolution of the lattice constant with particle size. The lattice parameters were determined from digitized HREM images by means of digital image processing. The data were calculated from {111} lattice plane fringes. Possible changes of (200) lattice planes as derived from electron diffraction studies [41] were not considered. The evaluation of lattice spacings directly from HREM images or from the corresponding diffractograms (*i.e.* their Fourier transform) resulted in data with statistical error of 0.25%. The determination of lattice parameters by HREM was in more detail described elsewhere [42,43]. This procedure was used to obtain the lattice constant of free and embedded Ag particles of different size.

Figure 4 represents the evolution of the lattice constant with the Ag particle reciprocal radius for both cases. For comparison, the previously reported results evaluated from electron diffraction data ({111} planes) [41] for free Ag particles are shown additionally (solid triangles) in Figure 4a. They are in good agreement with our results. It is worth to point out that the lattice contraction behavior of Ag particles in argon matrix is almost the same as that of free Ag particles. The corresponding results obtained by extended X-ray-absorption fine structure investigations [44] are also shown (open circles) in Figure 4a. This means that the size evolution of the Mie resonance for Ag particles in argon should be similar to that for free Ag particles since both adopt nearly the same A value of the free path effect (see next section). The lattice constant of particles is smaller than that of the bulk material. From the linear regression (solid line in Fig. 4) we get, according to equation (10), the surface (or interface) stress values 6.3 ± 1.3 N/m and 4.5 ± 1.3 N/m for the free and embedded Ag particles, respectively, by using the value $K = 9.93 \times 10^{-12}$ m^2/N [45].

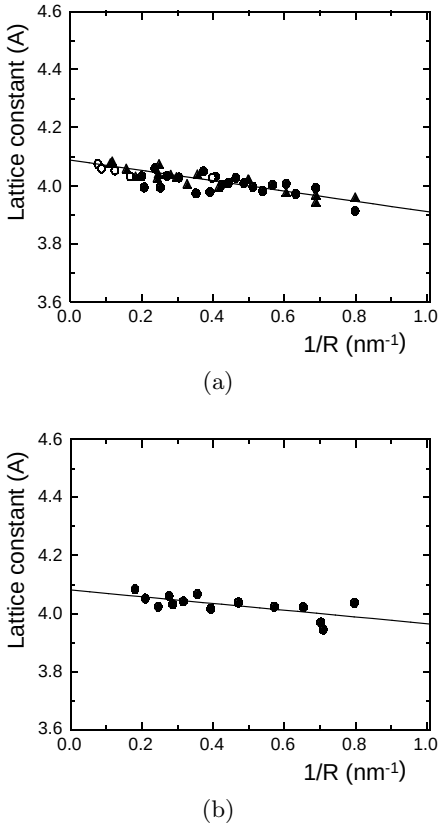

Fig. 4. Lattice constant *versus* reciprocal radius $1/R$ for (a) free silver particles (solid circles and solid triangles [41]) and particles in argon (open circle [44]) and (b) for the particles embedded in glass (solid circles).

4 Discussion

Now we can quantitatively discuss the importance of lattice contraction in the Mie resonance shift for Ag particles, based on the surface stress results presented above and the parameter values given in the previous section. In comparing our model predictions with experimental results, we must consider the effect of the size distribution of the particles, which mainly results in a broadening of the resonance band. The resonance position, however, is found remarkably insensitive to the occurrence of a size distribution with log-normal, Gaussian or triangular shape function of narrow width [46]. Therefore, the effect of the size distribution was mostly neglected in the literature on the particle size evolution of the Mie resonance [21,22,47]. Accordingly, under the assumption that the particle size distribution is sufficiently narrow for the reported experiments, we consider instead the mean particle size in our discussion.

4.1 Thermal effects

The blue shift of the Mie resonance originating according to equation (14) from the lattice contraction induced by temperature reduction is qualitatively in agreement with the classical results reported by Kreibig [29]. In his investigation of the plasmon resonance for two sizes of silver particles ($R = 1.7$ nm and 5.75 nm) [48] in glass measured at 300 K and 1.5 K, respectively, (see Fig. 4 in Ref. [29]), it was shown that although different sizes induced obvious changes of resonance width and shape, a significant decrease of the measuring temperature resulted in only a slight blue-shift of the peak position of just about 2 nm for both, the smaller and the larger particles. This means that different particle sizes did not yield measurable differences of the resonance shift, which is in good agreement with our results. A quantitative access in terms of the temperature change may consider the volume contraction $\Delta V/V$ of Ag particles in glass that was given to be 1.01×10^{-2} [29]. Applying this value to equation (14) we obtain $\Delta\omega_{\rm L} = 0.015$ eV (2 nm) in accordance with the experimental result. Therefore, the blue-shift due to the temperature reduction can be attributed to the accompanying lattice contraction.

4.2 Free Ag particles

As we have already mentioned, the size evolution of the lattice contraction is nearly the same for Ag particles in argon matrix as in vacuum. So, we consider both together [16], since also the size evolution of the Mie resonance should be nearly the same for both. Using the parameter values $A = 0.25$ and 0.3 for vacuum and argon, respectively and $f = 6.3$ N/m^2, according to the method and related equations presented above, we obtain the size evolution of the Mie frequency for Ag particles in vacuum, see curve (a) of Figure 5, and argon, see curve (b) of Figure 5, which have nearly the same slope. These calculations indicate the linear relation of the Mie frequency to $1/R$ for isolated silver particles in vacuum and argon, in agreement with previous experimental results [49] for Ag particles of narrow size distribution in argon, although quantitatively, there is a difference. This may be due to a certain porosity [21] at the metal/matrix interface as found for codeposited systems such as Ag/argon. Therefore, we additionally consider the effects of local porosity that may be simplified as a perfect "vacuum shell" of thickness $d_{\rm m}$ [22] around the cluster, which is a measure of the local porosity. Thus we can use instead of equation (2) a Mie-like formula appropriate to coated spheres [3]:

$$\sigma_{\rm abs} = \frac{18\pi\varepsilon_{\rm m}^{1/2}V_0}{\lambda} \times {\rm Im}\left[\frac{(\varepsilon_{\rm V}-\varepsilon_{\rm m})(\varepsilon+2\varepsilon_{\rm V})+\Gamma(\varepsilon-\varepsilon_{\rm V})(\varepsilon_{\rm m}+2\varepsilon_{\rm V})}{(\varepsilon_{\rm V}+2\varepsilon_{\rm m})(\varepsilon+2\varepsilon_{\rm V})+2\Gamma(\varepsilon-\varepsilon_{\rm V})(\varepsilon_{\rm V}-\varepsilon_{\rm m})}\right] \quad (15)$$

to determine the size evolution of the Mie resonance for Ag/argon, by taking $d_{\rm m} = 0.25$ nm [21], where $\Gamma = [R/(R+d_{\rm m})]^3$, $\varepsilon_{\rm V}$ is the dielectric constant of vacuum. The result shown in curve (c) of Figure 5 indicates a good agreement.

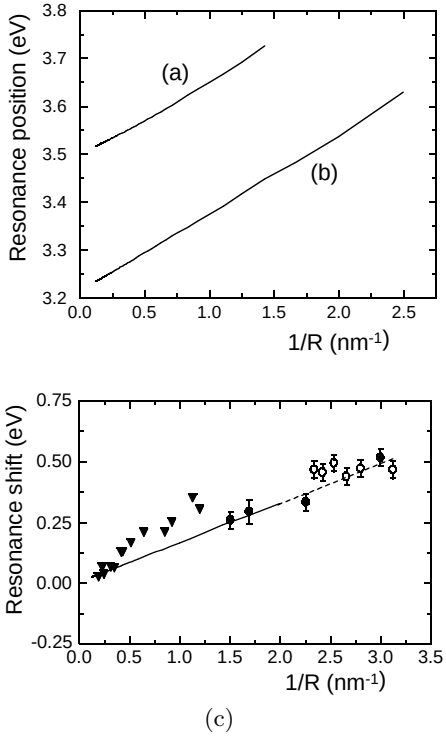

(c)

Fig. 5. Theoretical size evolution of the Mie resonance for Ag particles (a) in vacuum and (b) fully embedded in argon; curve (c): theoretical result by additionally considering the effects of local porosity (see text). Triangles: experimental results for Ag particles in argon [46].

Since we do not have enough experimental data available for free Ag particles in vacuum we apply our model to the results of Hövel *et al.* [32]. Figure 6 contains the optical spectrum for free Ag particles of 1 nm radius in vacuum, drawn up according to Figure 4 of reference [32], see curve (a). These particles produced by means of a special cluster source are nearly monodispers [32,50]. The resonance occurs at $\omega_0 = 3.65$ eV, but the authors' calculation, taking into account only the free path effect from equation (2) combined with equations (3, 7) for $a = a_0$, yields a spectrum peaking at about 0.17 eV lower, see curve (b) in Figure 6 [51]. This significant difference was attributed by Hövel *et al.* to the size dependence of the $4d{-}5sp$ interband transition edge, or a possible lattice contraction, but the latter issue was not treated in detail and quantitatively. We propose to explain this blue-shift quantitatively according to the model presented in this paper. When taking $A = 0.25$, $R = 1$ nm, and combining equations (3, 4, 7, 10), we obtain from equation (2), the corresponding optical absorption spectrum for free Ag particles in vacuum, shown as curve (c) in Figure 6, which is in good agreement with the experimental measurement. These findings indicate that the blue-shift with respect to large sized Ag particles of the surface plasmon resonance

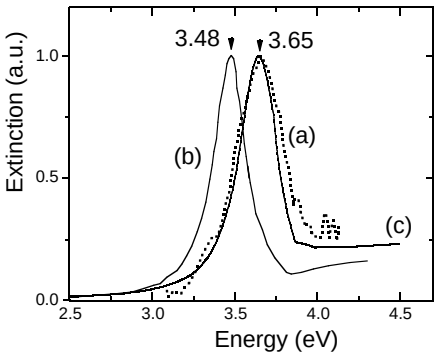

Fig. 6. Optical absorption spectra of free Ag particles (R = 1 nm) in vacuum. (a) Experimental results [32]; (b) theoretical result obtained by only considering the free path effect (A = 0.25) [32]; (c) theoretical spectrum obtained by consideration of both, lattice contraction and free path effect ($A = 0.25$).

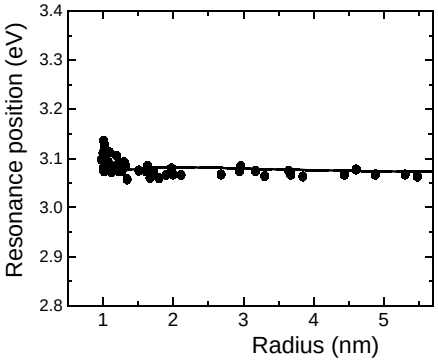

Fig. 7. Position of the plasmon peak of silver particles in glass *versus* the particle radius. Solid circles: experimental data [50], solid line: theoretical result from equation (8).

in vacuum and argon is induced by a lattice contraction resulting in an increase of the free electron density, what means, it is classical in origin.

4.3 Embedded Ag particles

For Ag particles embedded in glass, there are enough experimental data available. The size evolution of the Mie resonance, obtained by using $\varepsilon_{\rm m} = 2.25$, $A = 1.0$, $f = 4.5$ N/m, from equation (8), is shown in Figure 7 (solid line). No obvious shift or quasi-size-independent evolution is exhibited. The corresponding experimental results [50] are also included (solid circles) in Figure 7. Here, the size distribution is the same as mentioned in Section 4.1 [11,48]. Both are in good agreement. Although the contribution of lattice contraction to the Mie resonance shift for Ag particles in glass is larger than in argon and vacuum, its free path effect is the most significant because of the largest A value. From these findings the Mie frequency follows to be independent of the particle radius down to nearly 1 nm (see Fig. 6). For particles in vacuum and argon, however, since the free path effect is very weak (low A value), the corresponding Mie resonance adopts a

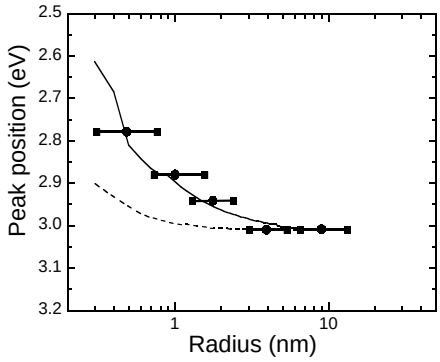

Fig. 8. Optical absorption peak position as a function of the Ag particle radius in stained glass. Data points: experimentally determined values given by Smithard [8]; solid lines: theoretically calculated results assuming $f = -4.5$ N/m and $A = 1$ ($\varepsilon_{\rm m} = 2.56$); dash line: calculated by only considering the free path effect (*i.e.*, $f = 0$).

stronger dependence on the particle size due to the lattice contraction.

So far, most of the studies performed on silver particles have pointed out the blue-shift or no obvious shift of the Mie resonance with decreasing particle size. There are only few reports about a red-shift of the resonance peak [8,10]. A typical result was given by Smithard [8]. He found a significant red-shift for Ag particles of apparently quite sharp size distribution [7] in glass when the radii were smaller than 4 nm, as shown in Figure 8 (data points). This abnormal shift was explained by some authors. Ganiere *et al.* [9] calculated the position of the Mie resonance using the quantum mechanical theory of Kawabata and Kubo. Apell and Ljungbert [52] made corrections to the classical situation by considering a nonlocal response with a smoothly varying surface profile [53,54]. These corrections enter as two lengths $d_{\rm r}(\omega)$ and $d_\theta(\omega)$, which are measures of the nonlocality range [55]. However, till now the question remains open and the red-shift origin is still not clear completely. Here, we give an alternative explanation based on the model presented in this paper.

As mentioned in the previous section, when the interface stress of Ag particles embedded in a medium is small enough or negative (*i.e.*, lattice dilatation with reduction of particle size), a red-shift of the Mie resonance can be predicted. For this case, quantitatively, if taking $f = -4.5$ N/m, $A = 1$ and $\varepsilon_{\rm m} = 2.56$ [7], we obtain a very good agreement between the model and experimental results, as shown by the solid line in Figure 8, where the result from only considering the free-path effect is included for comparison (dashed line).

Generally, the lattice parameter of particles is expected to diminish with decreasing size. There are, however, some reports in the literature on lattice dilatation [56] and negative interface stress of up to -5.33 N/m [57]. Our previous studies [40,42,43,58] indicated that different synthesis conditions and surrounding media for Ag particles result in different amounts of interface stress. Recently, we have found by HREM and extended X-ray absorption fine

structure studies a size-dependent lattice dilatation for Ag particles in silicate glass subjected to specific synthesis conditions and subsequent thermal treatment [59]. Therefore, it may be reasonable to assume that the red-shift reported by Smithard is due to a corresponding lattice dilatation of the Ag particles caused by thermally induced tensile stresses exerted by the glass matrix.

5 Conclusion

In the frame of classical theory, a model was presented by combining the lattice parameter variation of Ag particles and the free path effect of electrons to predict the size evolution of the Mie resonance for free and embedded Ag particle. The model revealed that the Mie resonance is influenced mainly by the size dependent lattice contraction, which results in a blue-shift, and the free path effect, which leads to a red-shift. The size evolution of the resonance is the net result of the competition between both opposite trends. Calculations exhibit that the contribution of the lattice contraction to the Mie resonance shift is weakly dependent on the particle size ($R > 1.0$ nm) and the dielectric constants of the surrounding media, but subject to the roughly linear relation with the extent of the volume contraction of Ag particles. Because of the effect of the core electron dielectric function, a larger dielectric constant value of the surrounding medium has a comparably larger influence on the resonance shift induced by lattice contraction. Based on the lattice contraction measurements, which exhibit a linear relation of the lattice constant with the reciprocal Ag particle radius, model calculations proved that the size evolution of the Mie resonance for isolated Ag particles in vacuum and argon obeys the linear relation of $1/R$ in the size range studied. For the particles embedded in glass, however, due to the strong free path effect that balances the contribution of the lattice contraction, the Mie resonance is independent of the particle radius down to near 1 nm. All the predictions are quantitatively in agreement with the previous experimental results. Our study indicates that for isolated Ag particles in vacuum or argon the lattice contraction plays an important role in the size evolution of the Mie resonance due to their weak free path effect and strong surface stress. In addition, the abnormal red-shift of the resonance with reduction of Ag particle size may mainly be attributed to the lattice dilatation of particles.

References

1. A.E. Hughes, S.C. Jain, Adv. Phys. **28**, 717 (1979).
2. W.P. Halperin, Rev. Mod. Phys. **58**, 533 (1986).
3. U. Kreibig, M. Vollmer, *Optical Properties of Metal Clusters* (Springer, New York, 1995).
4. G. Mie, Ann. Phys. (Leipzig) **25**, 377 (1908).
5. K.P. Charle, W. Schulze, B. Winter, Z. Phys. D **12**, 471 (1989).
6. G.W. Arnold, J.A. Borders, J. Appl. Phys. **48**, 1488 (1977).
7. M.A. Smithard, R. Dupree, Phys. Stat. Sol. (a) **11**, 695 (1972).
8. M.A. Smithard, Solid State Commun. **13**, 153 (1973).
9. J.D. Ganiere, R. Rechsteuner, M.A. Smithard, Solid State Commun. **16**, 113 (1975).
10. K.J. Berg, A. Berg, H. Hofmeister, Z. Phys. D **20**, 309 (1991).
11. L. Genzel, T.P. Martin, U. Kreibig, Z. Phys. B **21**, 339 (1975).
12. H. Abe, W. Schulze, B. Tesche, Chem. Phys. **47**, 95 (1980).
13. Y. Borensztein, P. De Andres, R. Monreal, T. Lopez-Rios, F. Flores, Phys. Rev. B **33**, 2828 (1986).
14. W.A. de Heer, Rev. Mod. Phys. **65**, 611 (1993) and references therein.
15. S. Fedrigo, W. Harbich, J. Buttet, Phys. Rev. B **47**, 10706 (1993).
16. A. Liebsch, Phys. Rev. B **48**, 11317 (1993).
17. V.V. Kresin, Phys. Rev. B **51**, 1844 (1995).
18. L. Serra, A. Rubio, Z. Phys. D **40**, 262 (1997).
19. F. Cocchini, F. Bassani, M. Bourg, Surf. Sci. **156**, 851 (1985).
20. Wen Chu Huang, Juh Tzeng Lue, Phys. Rev. B **49**, 17279 (1994).
21. J. Lerme, B. Palpant, B. Prevel, M. Pellarin, M. Treilleux, J.L. Vialle, A. Perez, M. Broyer, Phys. Rev. Lett. **80**, 5105 (1998).
22. J. Lerme, B. Palpant, B. Prevel, E. Cottancin, M. Pellarin, M. Treilleux, J.L. Vialle, A. Perez, M. Broyer, Eur. Phys. J. D **4**, 95 (1998).
23. J. Crowell, R.H. Ritchie, Phys. Rev. **172**, 436 (1968).
24. F. Fujimoto, K. Komaki, J. Phys. Soc. Jap. **25**, 1679 (1968).
25. N. Barberan, J. Bausells, Phys. Rev. B **31**, 6354 (1985).
26. M. Achehce, C. Colliex, P. Trebbia, Scanning Electron Microsc. **I**, 25 (1986).
27. M. Acheche, C. Colliex, H. Kohl, A. Nourtier, P. Trebbia, Ultramicroscopy **20**, 99 (1986).
28. Z.L. Wang, Micron **27**, 265 (1996).
29. U. Kreibig, J. Phys. F: Met. Phys. **4**, 999 (1974).
30. R.D. Averitt, D. Sakar, N.J. Halas, Phys. Rev. Lett. **78**, 4217 (1997).
31. U. Kreibig, L. Genzel, Surf. Sci. **156**, 678 (1985).
32. H. Hövel, S. Fritz, A. Hilger, U. Kreibig, M. Vollmer, Phys. Rev. B **48**, 18178 (1993).
33. C.W. Mays, J.S. Vermaak, D. Kuhlmann-Wilsdorf, Surf. Sci. **12**, 134 (1968).
34. P.B. Johnson, R.W. Christy, Phys. Rev. B **16**, 4370 (1972).
35. H. Ehrenreich, H.R. Philipp, Phys. Rev. **128**, 1622 (1962).
36. A. Liebsch, Phys. Rev. Lett. **71**, 145 (1993).
37. B.N.J. Persson, Surf. Sci. **281**, 153 (1993).
38. K.-P. Charle, W. Schulze, B. Winter, Z. Phys. D **12**, 471 (1989).
39. The results in Figure 2 were obtained directly from calculations based on equation (2) according to the definition of the contribution of lattice contraction in agreement with equation (8).
40. M. Dubiel, H. Hofmeister, E. Schurig, Recent. Res. Devel. Appl. Phys. **1**, 69 (1998).
41. H.J. Wasserman, J.S. Vermaak, Surf. Sci. **22**, 164 (1970).
42. H. Hofmeister, M. Dubiel, H. Goj, S. Thiel, J. Microsc. **177**, 331 (1995).
43. M. Dubiel, H. Hofmeister, S. Thiel, Surf. Rev. Lett. **3**, 1083 (1996).
44. P.A. Montano, W. Schulze, B. Tesche, G.K. Shenoy, T.I. Morrison, Phys. Rev. B **30**, 672 (1984).

45. C. Kittel, *Introduction to Solid State Physics*, 7th edn. (John Wiley & Sons, Inc., New York, 1996), p. 59.
46. C.G. Granquist, O. Hunderi, Phys. Rev. B **16**, 3513 (1977).
47. B. Palpant, P. Prevel, J. Lerme, E. Cottancin, M. Pellarin, M. Treilleux, A. Perez, J.L. Vialle, M. Broyer, Phys. Rev. B **57**, 1963 (1998).
48. The size distribution is fairly narrow, 74% of the particles have radii R_i with $0.7 \leq R_i \leq 1.3$.
49. K.-P. Charle, F. Frank, W. Schulze, Ber. Bunsenges. Phys. Chem. **88**, 350 (1984).
50. U. Kreibig, M. Gartz, A. Hilger, H. Hövel, in *Advances in Metal and Semiconductor Clusters*, edited by M. Duncan (JAI Press, Stanford, 1998), Vol. 4, p. 345.
51. The peak position is around 3.48 eV, (see Fig. 4 in Ref. [32]), due to the red shift induced by the free path effect instead of 3.50 eV which is the position for large sized particles, although the authors in reference [32] took an approximate value of 3.50 eV, or 0.15 eV lower than the experimental value.
52. P. Apell, A. Ljungbert, Solid State Commun. **44**, 1367 (1982).
53. P. Apell, A. Ljungbert, Phys. Scripta **26**, 113 (1982).
54. S.P. Apell, J. Giraldo, S. Lundqvist, Phase Trans. **24-26**, 577 (1990).
55. W. Ekardt, Phys. Rev. B **29**, 1558 (1984).
56. C. Goyhenex, C.R. Henry, J. Urban, Philos. Mag. A **69**, 1073 (1994).
57. H. Hofmeister, F. Huisken, B. Kohn, Eur. Phys. J. D **9**, 137 (1999).
58. H. Hofmeister, S. Thiel, M. Dubiel, E. Schurig, Appl. Phys. Lett. **70**, 1694 (1997).
59. M. Dubiel, S. Brunsch, C. Mohr, H. Hofmeister, *Proceedings of XVIII Int. Cong. on Glass*, San Francisco, 1998, edited by M.K. Choudhary, N.T. Huff, C.H. Drummond III, the American Ceramic Society, Westerville, Ohio 1998, session C1, pp. 119-124, on CD-ROM.

EPJ D proofs
(will be inserted by the editor)

Erratum

Importance of lattice contraction in surface plasmon resonance shift for free and embedded silver particles

W. Cai[1], H. Hofmeister[1], and M. Dubiel[2]

[1] Max Planck Institute of Microstructure Physics, Weinberg 2, 06120 Halle, Germany
[2] Martin Luther University of Halle-Wittenberg, Department of Physics, Friedemann-Bach-Platz 6, 06108 Halle, Germany

Eur. Phys. J. D **13**, 245–253 (2001)

Figure 5 was erroneous. To be in agreement with the text, this figure should be replaced by the the following one.

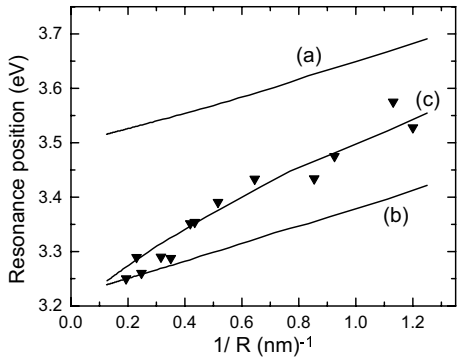

Fig. 5. Theoretical size evolution of the Mie resonance for Ag particles (a) in vacuum and (b) fully embedded in argon; curve (c): theoretical result by additionally considering the effects of local porosity (see text). Triangles: experimental results for Ag particles in argon [49].

[49] K.-P. Charle, F. Frank, W. Schulze, Ber. Bunsenges. Phys. Chem. **88**, 350 (1984).